Journal of Materials Processing Technology 225 (2015) 347–356

Contents lists available at ScienceDirect

Journal of Materials Processing Technology

journal homepage: www.elsevier.com/locate/jmatprotec

Influence of process parameters on friction stir spot welded aluminum joints by various threaded tools

Yuan-Ching Lin*, Jiun-Nan Chen

Department of Mechanical Engineering, National Taiwan University of Science and Technology, 43, Keelung Road, Section 4, Taipei 10673 Taiwan, ROC

ARTICLE INFO

Article history:
Received 28 March 2015
Received in revised form 18 June 2015
Accepted 20 June 2015
Available online 24 June 2015

Keywords:
Friction stir spot welding
Aluminum alloy
Material flow
Joint strength

ABSTRACT

The flow behavior and strength of joints created using three stirring tools, with right-handed threads at different locations on their cylindrical pins, were investigated. The threading locations on the tools significantly influenced the evolution of the stir zone in the welds and caused material intermixture in various degrees at varying plunging depths. Failure joints were observed in the welds without tool rotation. Force measurements indicated that the highest torque was found in the welds at 900 rpm. Not much difference was observed in the axial force variation between the welds. The peak temperature was obtained at the measured point nearest to the tool shoulder. The maximum joint strength of over 6.5 kN was obtained in the 900 rpm weld with a 9 s dwell time.

1. Introduction

The conventional method for joining aluminum alloys, resistance spot welding (RSW), is quite complex because of their high thermal conductivity, consuming power and current (Florea et al., 2012). Welding defects such as pores and cracks may also be induced, decreasing the weld strength. Therefore, FSSW seems to be a favorable spot welding process for joining aluminum alloys.

Badarinarayan et al. (2009b) reported that hook geometry played an important role in determining the static strength of welds. In addition, tool-pin geometry significantly affected the hook shape. Babu et al. (2013) proposed that the mechanical performance of FSSW is mainly governed by its geometrical features (hook height and bond width). Zhao et al. (2014) indicated that the tensile shear failure load of the FSSW joint is dependent on the hook geometry. Material flow morphology affects the joint strength because of the hook shape, and hook formation would be detrimental to weld strength, as reported by Badarinarayan et al. (2009a). Thus, hook formation is worthy of investigation by observation of the evolution of material flow during the plunging period.

Su et al. (2007) proposed that dissimilar intermixing during the dwell period results from the incorporation of upper (Al 5754) and lower (Al 6111) sheet materials at the top of the thread on the rotating pin and its rapid transfer downward into the SZ via threads on the pin. Fujimoto et al. (2008) indicated that the material near the pin was driven downward by the threads, and the material originally from the lower sheet was pushed outward as well as upward. Similarly, Lin et al. (2013) reported that threads on a cylindrical pin could increase the axial material flow during FSSW. The material flows downward along threads while the pin is rotated in the appropriate direction and then discharges at the pin tip to form a circulating material flow. The pin's bottom and top are the material entrance and exit, respectively. Fujimoto et al. (2009) indicated that the threads on the probe surface are important for producing plastic flow in the thickness direction during FSSW. Tozaki et al. (2007) performed FSSW using tools with three different probe lengths, suggesting that joint strength is proportional to probe length. Yuan et al. (2011) investigated the effect of distinct tool rotational speeds and directions on lap-shear separation load. The highest load was achieved in the upper sheet fracture (USF) mode.

The studies mentioned in the above paragraphs showed that tool geometry is a crucial characteristic for controlling the material flow evolution in FSSW. The effect of threading locations on cylindrical pins has not yet been discussed. Thus, tools with three threading locations on the cylindrical pins were applied to the execution of FSSW, trying to alter the material flow characteristics such as SZ height and hook morphology. Later, tension-shear tests were carried out to evaluate the joint strength. Moreover, the evolution of material flow and hook formation during the plunging period was traced step by step.

* Corresponding author. Fax: +886 27376460.
E-mail address: yclin@mail.ntust.edu.tw (Y.-C. Lin).

http://dx.doi.org/10.1016/j.jmatprotec.2015.06.024
0924-0136/

Table 1
Chemical composition of A5052-H32 and A6061-T6.

Element (wt.%)	Si	Fe	Cu	Mn	Mg	Cr	Zn	Ti	Al
A5052-H32	0.10	0.27	0.02	0.06	2.38	0.19	0.01	0.01	Rem.
A6061-T6	0.72	0.38	0.21	0.10	1.00	0.14	0.09	0.03	Rem.

Table 2
Mechanical property of A5052-H32 and A6061-T6.

	Modulus of elasticity, E (GPa)	Yield strength, σ_y (MPa)	Ultimate tensile strength, σ_u (MPa)	Elongation, d (%)
A5052-H32	70.3	193	228	12
A6061-T6	68.9	276	310	12

2. Experimental

Workpieces of Al–Mg (A5052-H32) and Al–Mg–Si (A6061-T6) aluminum sheets were chosen as weld specimens in this study. Tables 1 and 2list the chemical composition and mechanical properties of A5052-H32 and A6061-T6 sheets, respectively. Prior to FSSW, the aluminum sheets were machined to dimensions of $70(L) \times 35(W) \times 1.6(H)\,mm^3$. Ultrasonic cleaning with an acetone bath was conducted to remove contamination from the surface of the sheets.

FSSW tools were made of JIS SKD61 hardened steel with a hardness of HRc 50. The tool had a 10° concave shoulder 12 mm in diameter, and a cylindrical pin 5 mm in diameter and 2.8 mm in length. On cylindrical pins, external M5 right-handed threads were machined at distinct locations on three parts, as shown in Fig. 1. After the B-tool reaches a set plunging depth of 2.8 mm, the sink and source of material are above the interface, whereas they are below the interface for the T-tool; for the M-tool, the sink is above the interface and the source is below.

Two FSSW experiments were conducted. The first experiment applied overlapped dissimilar sheets of A5052-H32 (upper) and A6061-T6 (lower) to observe the material flow of welds. The welds were cut perpendicular to the rolling direction of the sheets to observe the cross-sectional material flow. The cut cross-sectional specimens were cold-mounted and then grounded by wet paper and polished with Al_2O_3 suspension. Keller's reagent (380 mL H_2O + 10 mL HNO_3 + 6 mL HCl + 4 mL HF) was used to etch the specimens to reveal the microstructure of the welds. The second experiment used overlapped A5052-H32 sheets to investigate force and temperature variations during FSSW. The specimens were fixed with a steel anvil and FSSW experiments were performed with a CNC machine. Force measurement was carried out using a four-axis Kistler 9272 dynamometer associated with a four-channel Kistler 5070 charge amplifier. Simultaneously, using an NI 9213 device for data acquisition and LabVIEW software for data collection, the temperature variation was sensed and recorded at a sampling rate of 100 Hz. Prior to temperature measurement, thermocouples were covered with ceramic bars and inserted into specific locations to prevent contact between the sheets and thermocouples. *K*-type thermocouples as small as 0.5 mm in diameter were used to acquire rapid signal responses in a short processing time. The measuring locations in the welds are shown in Fig. 2. Following FSSW, tension-shear tests were performed using the MTS Insight™ testing apparatus at room temperature to evaluate the joint strength of the welded specimens with a mm^2 overlapped area. The pneumatic cross-head speed was fixed at 1 mm/min. The joint strengths of welds under various welding parameters were obtained by averaging the results from at least three individual replicates for ensuring experimental repeatability. Later, fractographic cross sections were observed to examine the fracture characteristics and fracture modes.

3. Results

Figs. 3–5 show the cross sections of welds made with B-, M-, and T-tools at various pin plunging depths, individually. Tool dwell time was set to zero to eliminate the material flow disturbance during dwell periods. The welds at the 0.6 mm and 1.2 mm plung-

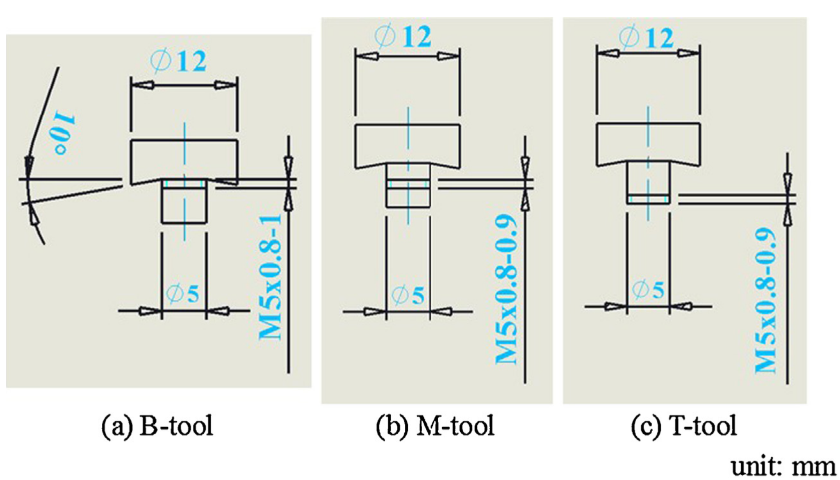

Fig. 1. Geometry and screw threads location of tools.